Higher-Order Array Decomposition Method for Arrays with Dielectric Substrates

Magnus Brandt-Møller[(1)(3)], Michael Mattes[(1)], Olav Breinbjerg[(2)], Min Zhou[(3)], and Erik Jørgensen[(3)]

[(1)] EMS, Technical University of Denmark, Kgs. Lyngby, Denmark, {magbran, mmattes}@dtu.dk
[(2)] ElMaReCo, Copenhagen, Denmark, olavbreinbjerg@outlook.com
[(3)] TICRA, Copenhagen, Denmark, {mbm, mz, ej}@ticra.com

***Abstract*—The Higher-Order Array Decomposition Method (HO-ADM) has been extended to regular arrays with dielectric substrates. To maintain the multi-level block-Toeplitz Method of Moments (MoM) matrix structure, internal equivalent currents are introduced, ensuring an FFT-accelerated matrix-vector product (MVP). Results demonstrate a tenfold reduction in computation time and lower memory consumption compared to an existing fast method, specifically for a 400-element array of PEC cylinders embedded in a dielectric substrate.**

I. Introduction

Modern array antenna designs are evolving towards configurations with densely packed elements, leading to electrically large structures characterized by prominent edge effects and substantial mutual coupling occurring. In the realm of array analysis, the use of surface integral equations solved via the full-wave Method of Moments (MoM) comprehensively accounts for mutual coupling and edge effects. This is nevertheless at the expense of a computational complexity and memory consumption which scales as $\mathcal{O}(N^2)$–$\mathcal{O}(N^3)$ and $\mathcal{O}(N^2)$, respectively, where N is the number of unknowns.

Several fast full-wave analysis techniques incorporating error-controllable approximations have been developed, including, but not limited to, the Multi-Level Fast Multipole Method (MLFMM) [1], the Adaptive Integral Method (AIM) [2], and the pre-corrected fast Fourier transform (pFFT) [3], which are able to significantly reduce memory consumption and computational complexity to as low as $\mathcal{O}(N \log N)$. While the MLFMM approximates long-range interactions using a hierarchical multilevel decomposition of the computational domain, the approximation of the AIM and pFFT methods lies in projecting basis functions (BFs) onto a regular grid.

Nevertheless, for regular arrays, the Array Decomposition Method (ADM) [4] offers a computational and memory scaling of $\mathcal{O}(N \log N)$ and $\mathcal{O}(N)$, respectively, without such approximations. Recently, the boundary integral part of ADM has been integrated with higher-order (HO) BFs, substantially reducing the number of unknowns for a specific accuracy while achieving a tenfold computational speed-up compared to first-order BFs [5]. The HO-ADM has been extended to electrically connected arrays [6] and arrays with non-identical elements [7]. However, thus far the HO-ADM has been unable to analyze connected array elements of finite thickness, such as arrays with a dielectric substrate. This paper proposes an extension to the HO-ADM, enabling it to handle connected array elements of finite thickness, including those with dielectrics.

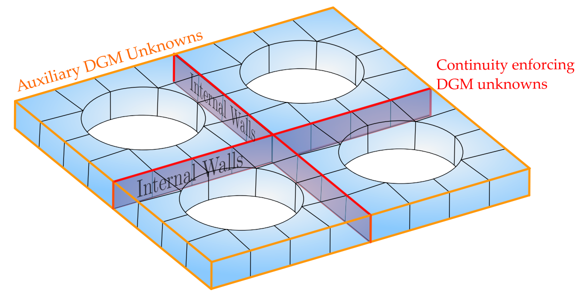

Fig. 1. A finite-thickness, electrically connected array structure on which equivalent electric and magnetic currents are placed on internal walls to make each array element identical from an electromagnetic perspective.

II. HO-ADM with Dielectric Substrates

The HO-ADM utilizes the multi-level block-Toeplitz (MBT) structure of the MoM matrix $\mathbf{A}$ for regular arrays, to enable an FFT-accelerated matrix-vector product (MVP). However, in case of electrically connected array elements of finite thickness, this MBT structure is lost because elements on the edge and inside of the array do not possess the same number, nor placement, of BFs. To overcome this problem, internal equivalent currents (IECs), together with the Discontinuous Galerkin Method [8] (DGM), and the Poggio-Miller-Chang-Harrington-Wu-Tsai (PMCHWT) formulation are employed to keep the MBT structure of $\mathbf{A}$, which in turn allows for an FFT-accelerated analysis of connected array elements with dielectric substrates.

More specifically, for a generic electrically connected array structure of finite thickness as shown in Fig. 1, equivalent electric and magnetic currents are added on both sides of the depicted internal walls. By letting these internal walls radiate into the background medium, just as the external lateral walls of the original structure, each element becomes identical from an electromagnetic perspective and the associated MoM matrix will again obtain the MBT structure, allowing the HO-ADM to be applied. Note, that the equivalent currents added on internal walls should not be part of the simulation, which would erroneously simulate their radiation into the background medium. To avoid this, currents on internal walls are excluded from the simulation by utilizing a constrained Krylov subspace technique [7] to hide the internal walls from the iterative solvers perspective. The DGM is used, as described in [6], to place half roof-top BFs and to ensure current continuity

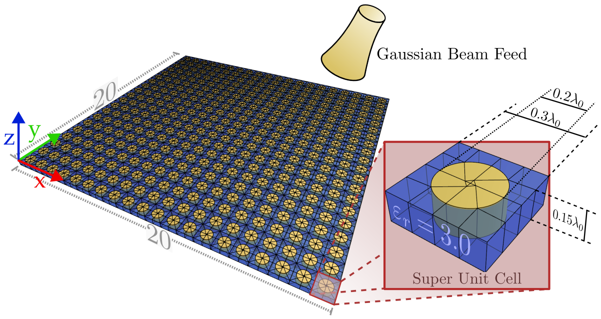

Fig. 2. A $20 \times 20 = 400$-element array of PEC cylinders with a diameter of $0.2\lambda_0$ embedded in a $0.15\lambda_0$-thick dielectric layer with a permittivity of $\varepsilon_r = 3.0$, including dimensions and mesh used for analysis in the HO-ADM.

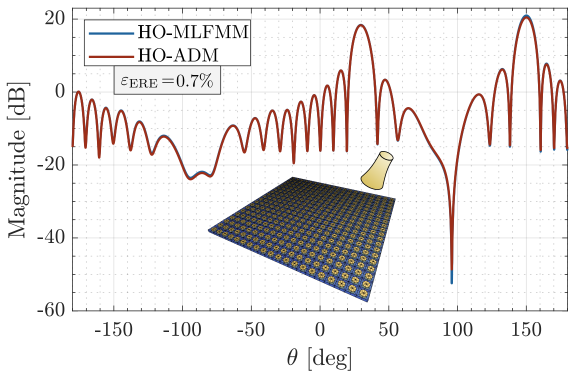

Fig. 3. Co-pol scattered far-field $\phi = 180°$-cut for an obliquely incident ($\theta_i = 30°, \phi_i = 0°$) y-polarized Gaussian beam feed on the $20 \times 20 = 400$-element array in Fig. 2, comparing the HO-ADM to HO-MLFMM.

over the edges where the individual elements are connected on the top and bottom surfaces (red lines in Fig. 1). Last but not least, to keep the MBT MoM matrix structure when using DGM, auxiliary DGM unknowns need to be placed on outer array elements on those edges (marked in orange) which would have been connected if that element had been completely surrounded by array elements.

III. Application Example

We consider a Gaussian beam illumination of 400 PEC cylinders with a diameter of $0.2\lambda_0$ embedded in a $0.15\lambda_0$-thick dielectric layer with a relative permittivity of $\varepsilon_r = 3.0$, as shown in Fig. 2, where λ_0 is the free-space wavelength. The array is illuminated by an obliquely incident y-polarized Gaussian beam with a field taper of -20 dB at $\theta = 30°$ from boresight.

In the HO-ADM, the structure is analyzed as a 20×20-element array of identical elements by using the IEC method described in Sec. II. The mesh comprises 28,800 quadrilateral mesh cells, resulting in $N = 422{,}400$ unknowns. In the HO-MLFMM, no internal walls are needed, resulting in a total of 22,720 mesh cells corresponding to $N = 267{,}520$ unknowns.

Table I shows the total computation time and memory consumption of HO-ADM and HO-MLFMM. It is seen that despite that HO-ADM uses nearly 60 % more unknowns, the total computation time for HO-ADM is more than an order of magnitude faster than HO-MLFMM. The memory consumption of HO-MLFMM is 7.0 GB while HO-ADM uses 5.1 GB. The lower memory consumption of HO-ADM is mainly due to the use of a specialized low-memory preconditioner in HO-ADM which takes into account known redundancies. Note also that HO-MLFMM is a general solver for arbitrary structures, whereas HO-ADM is specifically designed for arrays.

TABLE I
Comparison of solution time and memory consumption on a laptop (Intel® Core® i7-9850H CPU @ 2.6 GHz with 6 cores).

Method	Total Simulation Time	Memory Consumption	Number of Iterations
HO-MLFMM	2 h 12 min	7.0 GB	149
HO-ADM	11 min	5.1 GB	361

Fig. 3 shows the co-polar scattered far-field calculated with the HO-ADM and the HO-MLFMM for a $\phi = 180°$-cut which shows an equivalent relative error $\varepsilon_{\mathrm{ERE}}$ of 0.7 % over the entire region of 360°. A similar equivalent relative error is observed in the $\phi = 45°$ and $\phi = 90°$ planes.

IV. Conclusion

We presented an extended Higher-Order Array Decomposition Method capable of analyzing connected arrays of finite thickness with dielectric substrates and applied it to a $20 \times 20 = 400$-element array of PEC cylinders embedded in a dielectric substrate. The results show more than an order of magnitude computational speed-up compared to an already fast HO-MFLMM implementation while maintaining a lower memory consumption.

References

[1] O. Borries, P. Meincke, E. Jørgensen, and P. C. Hansen, "Multilevel fast multipole method for higher order discretizations," *IEEE Trans. Antennas Propag.*, vol. 62, no. 9, pp. 4695–4705, 2014.

[2] S. Sharma and P. Triverio, "AIMx: an extended adaptive integral method for the fast electromagnetic modeling of complex structures," *IEEE Trans. Antennas Propag.*, vol. 69, no. 12, pp. 8603–8617, 2021.

[3] J. White, J. Phillips, and T. Korsmeyer, "Comparing precorrected-FFT and fast multipole algorithms for solving three-dimensional potential integral equations," in *Proc. Colo. Conf. Iter. Methods*, Colorado, CO, 1994, pp. 4–10.

[4] R. W. Kindt, K. Sertel, E. Topsakal, and J. L. Volakis, "Array decomposition method for the accurate analysis of finite arrays," *IEEE Trans. Antennas Propag.*, vol. 51, no. 6, pp. 1364–1372, 2003.

[5] M. Brandt-Møller, M. Mattes, O. Breinbjerg, M. Zhou, and O. Borries, "Array decomposition method for arbitrary-element regular arrays using higher order basis functions," *IEEE Antenn. Wirel. Propag. Lett.*, vol. 22, no. 1, pp. 24–28, 2023.

[6] M. Brandt-Møller, M. Mattes, O. Breinbjerg, M. Zhou, and E. Jørgensen, "Extended higher-order array decomposition method for fully populated or thinned array antennas and scatterers with connected elements," *IEEE Trans. Antennas Propag., to be published*, 2023.

[7] M. Brandt-Møller, M. Mattes, M. Zhou, E. Jørgensen, and O. Breinbjerg, "Extension of the higher-order array decomposition method for arrays with non-identical elements," in *Int. Conf. Electromagn. Adv. Appl.*, Venice, Italy, 2023, pp. 277–279.

[8] Z. Peng, K.-H. Lim, and J.-F. Lee, "A discontinuous Galerkin surface integral equation method for electromagnetic wave scattering from non-penetrable targets," *IEEE Trans. Antennas Propag.*, vol. 61, no. 7, pp. 3617–3628, 2013.